

## Wireless charging system for electric bicycle application

Nguyen Thi Diep<sup>1</sup>, Nguyen Kien Trung<sup>2</sup>, Tran Trong Minh<sup>3</sup>

<sup>1,2</sup>Department of Industrial Automation, Hanoi University of Science and Technology, Viet Nam

<sup>1,3</sup>Department of Automation and Control Engineering Technology, Electric Power University, Viet Nam

---

### Article Info

#### Article history:

Received Dec 12, 2019

Revised Apr 26, 2020

Accepted May 21, 2020

---

#### Keywords:

CC charging

CV charging

Electric bicycle

LCC compensation circuit

Wireless charging

---

### ABSTRACT

This paper presents a design of the wireless charging system for e-bike applications. The double-side LCC compensation circuit is used to achieve high efficiency and reduce the volt-ampere rating. A new constant current/voltage (CC/CV) charging control method at the transmitter side is proposed to avoid dual side wireless communication. This paper also presents a simple method of estimating both the coupling coefficient and load impedance only from the transmitter side. A wireless charging system of 2.5kW is built. Error in the CC/CV charging mode is 3.3% and 1.12%, respectively. System efficiency reaches 92.1% in CC charging mode.

*This is an open access article under the [CC BY-SA](https://creativecommons.org/licenses/by-sa/4.0/) license.*



---

### Corresponding Author:

Nguyen Kien Trung,  
Department of Industrial Automation,  
Hanoi University of Science and Technology,  
No. 1 Dai Co Viet Road, Hai Ba Trung, Hanoi, Viet Nam.  
Email: trung.nguyenkien1@hust.edu.vn

---

## 1. INTRODUCTION

Recently, electric bicycles (e-bike) are widely used instead of the motorcycle to reduce air pollution in the world. The users are almost students and women. Therefore, a convenient and safe charging method is necessary. Based on wireless power transfer (WPT) technology, wireless charging systems could be done automatically and safely without any human contact with electricity [1-3].

In wireless charging systems, the power can be transferred from the transmitter side to the receiver side over a short air gap [4]. These systems have a low coupling coefficient leads to high reactive power and low energy transfer efficiency. Therefore, the compensation circuit is used to reduce reactive power and improve system efficiency. There are four basic compensation circuits, which are series-series, series-parallel, parallel-series, and parallel-parallel [5]. These compensations are simple, easy to design, and it is sensitive to the variation of parameters [6]. Besides, some other compensation circuits are used to improve efficiency as LCL, CLL, LCC compensation circuits. However, the LCL compensation circuit requires a large compensation inductance value, close to the coil's inductance value [7, 8]. A capacitor is added to the LCL compensation circuit to reduce the size, the cost of circuit components that creates an LCC compensation circuit [9]. Also, the LCC compensation circuit has resonant frequency independent of the coupling coefficient, load, and the soft-switching condition for the electronic devices reached [10-12]. In [13], The CLL/S compensation circuit is used to limit the inverter current. However, the parameters of the compensation circuit are relatively large that is difficult to design high power systems. Besides, efficiency is slightly lower than the double-sided LCC compensation circuit.

The other problem with wireless charging is that the CC/CV charging modes are required to achieve high charging efficiency and lithium-ion pin protection [14, 15]. Therefore, a proper charging control strategy is required. The charging control methods in the WPT system consists of three types: transmitter side control, receiver side control, and dual side control [16-18]. In these methods, the transmitter side control is preferred because it doesn't require any additional DC/DC converter. However, parameters as load, coupling coefficient must be known to control at the transmitter side. Moreover, in the wireless charging, the voltage/current of the battery varies during the charging process [5, 19]. Therefore, the battery is considered a variable load during charging. Besides, to high-efficiency charging, the e-bike must park in alignment with the transmitter to receive energy from the transmitter. However, that is not always possible. When e-bikes park in misalignment, the coupling coefficient also varies with each charging [20, 21]. In the wireless charging, these parameters are difficult to obtain without using wireless communications.

The CC/CV charging is performed by designing a hybrid compensation circuit in [22]. However, the system is complicated because it needs to add capacitors, inductors, and switches. In [23], the CC/CV is performed via AC switches that the system requests weak communication. However, it leads to control deviations when the communication signal jammed. In [24], the CC / CV charging achieved through coil and compensation circuit design. However, the design method is complicated. The switching frequency must switch between the CC and CV charging modes. In [25], the CC/CV charging has performed at only the primary side. However, the load estimation method is complicated, which used the quadrature transformation algorithm to measure active power. Also, the mutual inductance was not estimated resulting in inflexible control.

In this paper, the LCC compensation circuit is designed for both transmitter and receiver to high efficiency and small compensation circuit elements value. Then, a new CC/CV charging control method only on the transmitter side is implement that base on a new high accuracy estimation method of both parameters like the coupling coefficient and load. A 2.5 kW wireless charging system has built to verify the feasibility of the proposed method. Section 2 presents a system structure and LCC compensation circuit design. Section 3 presents the CC/CV charging control method. Section 4 presents the simulation and experimental results. Conclusions are given in section 5.

## 2. SYSTEM STRUCTURE AND LCC COMPENSATION CIRCUIT DESIGN

The wireless charging system structure is shown in Figure 1. At the transmitter side, the DC voltage is converted into a high-frequency alternating voltage by a single-phase inverter for the magnetic coupler. The transmitter side controller performs CC/CV charging control through measuring resonant current and inverter DC input power. The primary side LCC compensation circuit is used to reduce reactive power, and achieve soft switching for MOSFETs. Then, energy is transferred to the receiver side via the magnetic coupler. The receiver side LCC compensation circuit is used to maximize transfer efficiency. The obtained AC voltage on the receiver coil via the LCC compensation circuit is rectified and filtered to charge for the battery. At the transmitter side, the equivalent load, and the coupling coefficient are estimated. Then, the transmitter side controller is designed to control CC/CV charging modes.

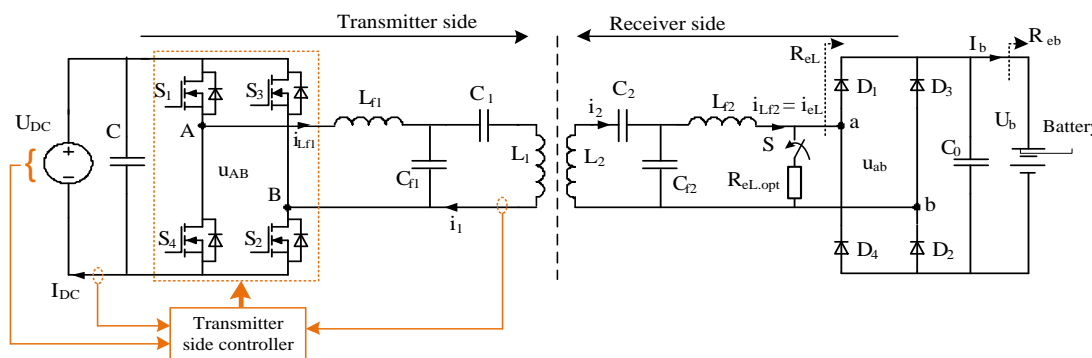


Figure 1. System structure diagram

When the battery charging process is slow, the battery can be modeled as a resistor  $R_{eb}$  which depends on the battery's state of charge [5, 25]. The battery equivalent resistance can be expressed as

$$R_{eb} = \frac{U_b}{I_b} \tag{1}$$

where  $U_b, I_b$  is the charging voltage, charging current, respectively. When ignoring power losses on rectifiers, the equivalent load resistance/current seen from the input of the rectifier is expressed as follows:

$$R_{eL} = \frac{8}{\pi^2} R_{eb} \tag{2}$$

$$I_{eL} = \frac{\pi}{2\sqrt{2}} I_b \tag{3}$$

When the inverter output voltage and rectifier input voltage are approximated as sinusoidal sources, the equivalent circuit is given in Figure 2. Where  $L_i$  is coil's self-inductance,  $M$  is the mutual inductance,  $L_{fi}, C_{fi}, C_i$  are compensation inductor and capacitors;  $i$  ( $i = 1,2$ ) index of parameters at the transmitter, receiver side, respectively.

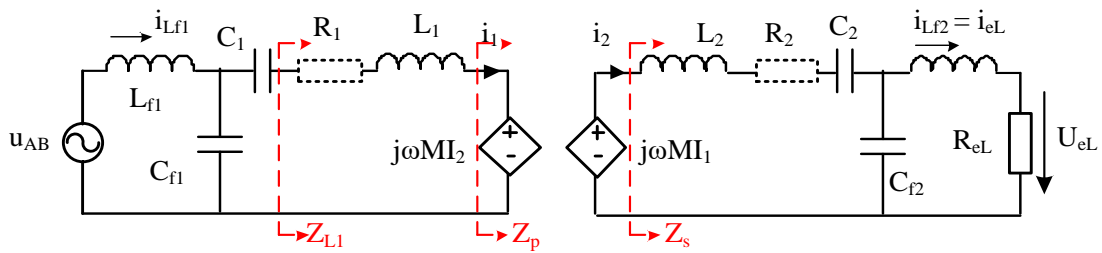


Figure 2. Equivalent circuit

Ignore internal resistance of coils, the fundamental harmonics approximation method is used to analyze the working principle of the resonant circuit. The transmitter and receiver coil have designed the same. Therefore, the following parameters are the same:

$$\begin{cases} L_1 = L_2 = L_i \\ L_{f1} = L_{f2} = L_{fi} \\ C_{f1} = C_{f2} = C_{fi} \end{cases} \tag{4}$$

The resonance frequency is design to be equal to the inverter switching frequency,  $\omega = 2\pi f_{sw}$ . Parameter's relationship in the resonant circuit is shown as follows.

$$C_{fi} = \frac{1}{\omega^2 L_{fi}} \tag{5}$$

$$C_i = \frac{1}{\omega^2 (L_i - L_{fi})} \tag{6}$$

The system output power can be expressed as follows

$$P_{out} = \frac{k L_i}{\omega L_{fi}^2} U_{AB} U_{ab} \tag{7}$$

Combine (5), (6), and (7), the compensation circuit parameters for the system are calculated and depicted in Table 1.

Table 1. System parameters

Parameter	Value	Parameter	Value
$P_{out}$	2.5 kW	$L_i$	110 $\mu$ H
$U_{DC}$	310 V	$R_i$	0.15 $\Omega$
$U_b$	330V – 420V	$C_i$	30.9 $\mu$ F
$f_{sw}$	40 kHz	$L_{fi}$	58.7 $\mu$ H
$R_{eL,opt}$	32 $\Omega$	$k$	0.25

### 3. PROPOSED TRANSMITTER SIDE CONTROLLER

#### 3.1. Theoretical analysis

Analyzing the circuit of Figure 2 when considering the internal resistance of the transmitter and receiver coils, the following relationships have drawn:

$$I_{eL} = \frac{\omega^2 k L_1 L_{f2}}{(\omega L_{f2})^2 + R_2 R_{eL}} I_1 \quad (8)$$

$$U_{eL} = \frac{\omega^2 k L_1 L_{f2}}{(\omega L_{f2})^2 + R_2 R_{eL}} R_{eL} I_1 \quad (9)$$

where  $R_i$  is coil internal resistances,  $I_1$  is resonant current on transmitter coil. At a fixed resonant frequency, from (8), (9) show that  $I_{eL}$ ,  $U_{eL}$  depends on  $k$ ,  $R_{eL}$ , and resonant current  $I_1$ . The coupling coefficient ( $k$ ) varies according to the position between the receiver and transmitter. The equivalent resistance ( $R_{eL}$ ) varies according to the battery charging state. If these parameters are estimated, the CC/CV charging is possible via transmitter side resonant current adjustment.

The resonant current is expressed by:

$$I_1 = -j\omega C_{f1} U_{AB} = -j \frac{U_{AB}}{\omega L_{f2}} \quad (10)$$

It shows that the transmitter resonant current  $I_1$  could be controlled by regulating inverter output voltage ( $U_{AB}$ ). The phase-shift method is used to adjust the RMS of  $U_{AB}$ . The PWM signals for  $S_1 \sim S_4$  and the phase-shift inverter output voltage is given in Figure 3. Through the first harmonic approximation,  $U_{AB}$  is given as [26]:

$$U_{AB} = \frac{2\sqrt{2}}{\pi} U_{DC} \cos \frac{\alpha}{2} \quad (11)$$

where  $\alpha$  is the phase-shift angle of the resonant inverter. The equations (8) to (11) show the ability to control CC / CV charging by adjusting the phase shift angle of the inverter.

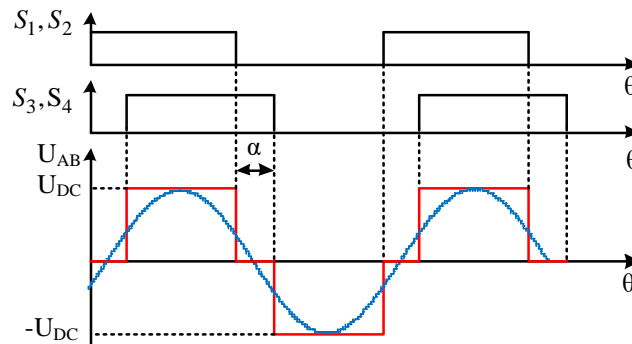


Figure 3. The PWM signals and phase-shift inverter output waveform

#### 3.2. Estimate the coupling coefficient and equivalent resistance from only the transmitter side

To make estimates of coupling coefficient and equivalent resistance only from the transmitter side, the circuit diagram Figure 2 is analyzed. The equivalent impedance of the receiver side seen into the receiver coil can be expressed:

$$Z_s = R_2 + \frac{(\omega L_{f2})^2}{R_{eL}} \quad (12)$$

The equivalent impedance of the transmitter side seen into the transmitter coil can be expressed:

$$Z_p = \frac{\omega^2 M^2}{Z_s} \quad (13)$$

The impedance of coil L1 can be expressed:

$$Z_{L1} = j\omega L_1 + R_1 + Z_p = j\omega L_1 + R_1 + \frac{\omega^2 M^2}{Z_s} \quad (14)$$

$$Re\{Z_{L1}\} = R_1 + \frac{\omega^2 M^2}{Z_s} = \frac{P_{L1}}{I_1^2} \quad (15)$$

If the losses on the compensation circuit elements are ignored, then:

$$Re\{Z_{L1}\} \approx \frac{P_{DC}}{I_1^2} \quad (16)$$

Where  $P_{DC}$  is inverter input DC power. Combining the equations (14) and (16), the coupling coefficient can be expressed:

$$k = \sqrt{\left(\frac{P_{DC}}{I_1^2} - R_1\right) \frac{Z_s}{(L_1 \omega)^2}} \quad (17)$$

Usually, the wireless charging system for e-bike is the static charging system. When starting charging, the vehicle position is fixed. Therefore, from equations (12) and (17), the parameters are estimated by the following two steps:

Step 1: When starting the charging process, the rectifier and battery are cut off and replaced by an optimum resistance ( $R_{L,opt}$ ) as shown in Figure 1. The coupling coefficient is estimated as (17). Then, the coupling coefficient value is remembered.

Step 2: After the coupling coefficient value has been collected, the optimum resistance load is cut off. The equivalent resistance value is estimated continuously during charging:

$$R_L = \frac{(\omega L_{f2})^2}{A - R_2} \text{ with } A = \frac{(\omega k L_1)^2}{\frac{P_{DC}}{I_1^2} - R_1} \quad (18)$$

Thus, by measuring the values of inverter input DC power and RMS of resonant current, the coupling coefficient and equivalent resistance are estimated.

### 3.3. Analysis of the proposed controller

The block diagram of the closed-loop control is given in Figure 4. The RMS of resonant current and input DC power of the inverter is measured. First, the coupling coefficient is estimated by (17) and remembered. Later, the equivalent load is estimated according to (18) during process CC/CV charging. Final, the value of equipment load current /voltage is calculated by (7), (8). The value of  $I_{eL}/U_{eL}$  is compared with  $I_{eL,ref}/U_{eL,ref}$ , the errors are fed into the PI (CC/CV) controller that creates the phase-shifted angle. The transfer function of the object is identified by PSIM simulation software. Then, CC/CV charging controller designed as bellow. Thus, the CC/CV charging process is performed.

$$G_{PI,CC}(s) = 2.6 + \frac{25 \cdot 10^4}{s} \quad (19)$$

$$G_{PI,CV}(s) = 0.01 + \frac{200}{s} \quad (20)$$

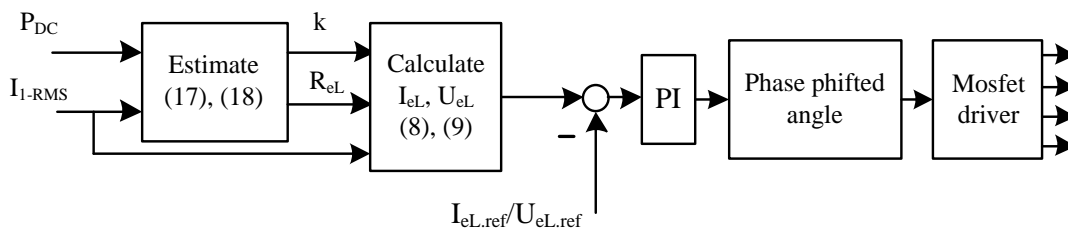


Figure 4. Closed-loop control block diagram

## 4. SIMULATION AND EXPERIMENT RESULTS

### 4.1. Simulation results

The circular coil structure is used to build the transmitter and receiver. When misalignment between the transmitter and receiver is variation, 2D/ 3D FEA simulation results of the coupling coefficient are shown in Figure 5. The results show that when misalignment between the transmitter and the receiver increases, the coupling coefficient decreases. The coupling coefficient equal to 0.25 is the highest when the transmitter and receiver align.

The wireless dynamic charging system is simulated by PSIM software to evaluate the proposed designs. Simulation model using the parameters given in Table 1. Figure 5b (k.est) show the estimation result of the coupling coefficient that estimated an error of less than 2%.

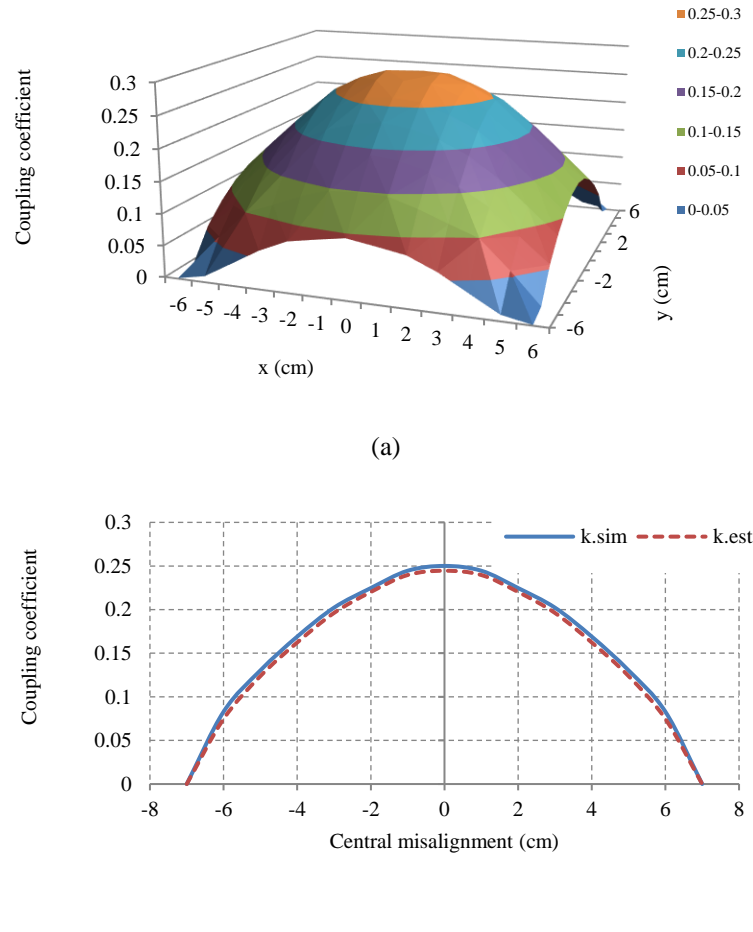


Figure 5. FEA simulation and estimation result of the coupling coefficient, (a) 3D simulation result, (b) 2D simulation and the estimation result

Figure 6 shows the results of a closed-loop simulation of the CC/CV charging process. The coupling coefficient is estimated at the beginning of the charging process. The value of equivalent load impedance is changed within a range of  $10\ \Omega$  to  $200\ \Omega$  during simulation, which corresponds to the charging state of the battery. Figure 6(a) shows CC charging mode simulation results with a reference value of 7.5 A. When the battery equivalent resistance ( $R_{eb}$ ) changes from  $15\ \Omega$  to  $25\ \Omega$ , simulation results indicate that: battery current is maintained to reference value with an error of 3.3%, battery voltage increases from 112V to 180V, estimated load resistance ( $R_{eb,est}$ ) varies from  $15.3\ \Omega$  to  $24.8\ \Omega$  with an estimation error of 1.4%. Figure 6(b) shows CV charging mode simulation results with a reference value of 400 V. When the battery equivalent resistance ( $R_{eb}$ ) changes from  $120\ \Omega$  to  $150\ \Omega$ , simulation results indicate that: battery voltage is maintained to reference value with an error of 1.12%, battery current decreases from 3,29 A to 2.64 A, estimated load resistance ( $R_{eb,est}$ ) varies from  $118\ \Omega$  to  $147\ \Omega$  with an estimation error of 1.8%.

Figure 7 gives waveform simulation results in the cases in Figure 6 at steady-state. Figure 7(a) shows to control the constant charging current in the simulation case, the phase-shift angle ( $\alpha$ ) reduces from  $28^\circ$  to

25°. Zero voltage switching for MOSFET is achieved with a maximum  $I_{off}$  of 2.5A. Figure 7(a) shows to control the constant charging voltage in the simulation case, the phase-shift angle increase from  $97^\circ$  to  $113^\circ$ . The voltage/current waveform of the MOSFET, in this case, is shown in Figure 7(c). The two legs of the inverter are operated in two different states of soft switching. The S1/S4 MOSFET operates in the zero voltage switching condition and S3/S2 MOSFET operates in the zero current switching condition. The S1/S4 has turn-off loss and S3/S2 has turn on-loss. The ZVS/ZCS condition depends on the phase-shift angle and load.

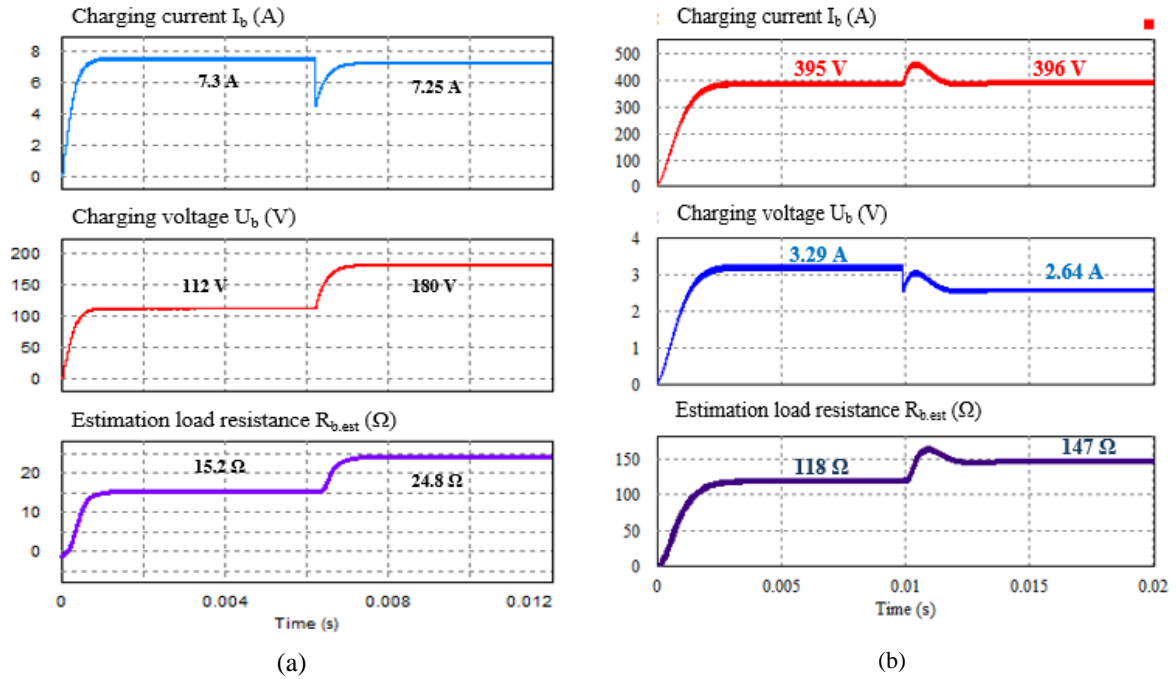


Figure 6. Closed-loop CC/CV charging simulation results, (a) CC charging, (b) CV charging

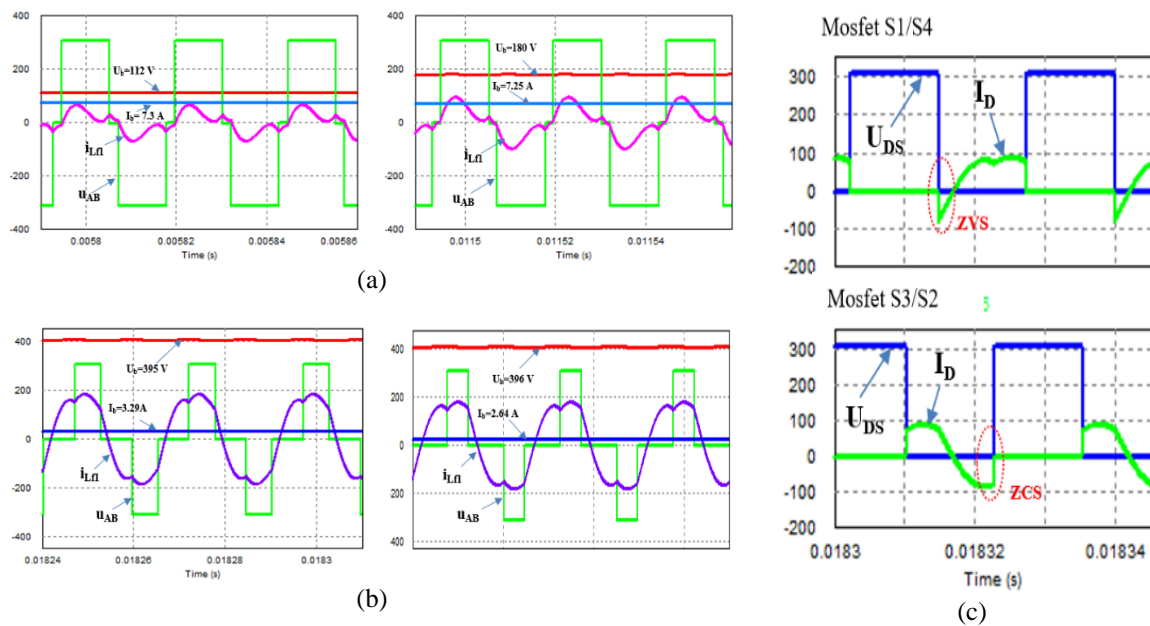


Figure 7. Simulation waveform, (a) CC charging mode, (b) CV charging mode, (c) Simulation waveform of MOSFET voltage/current in CV charging mode

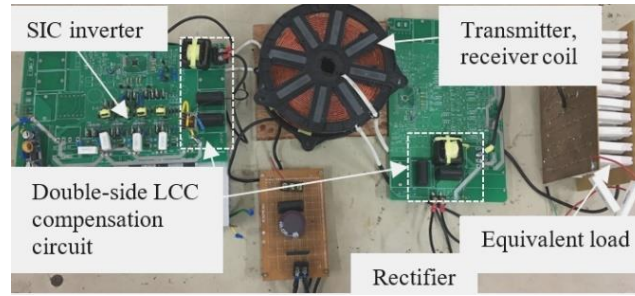


Figure 8. The wireless charging system experimental setup

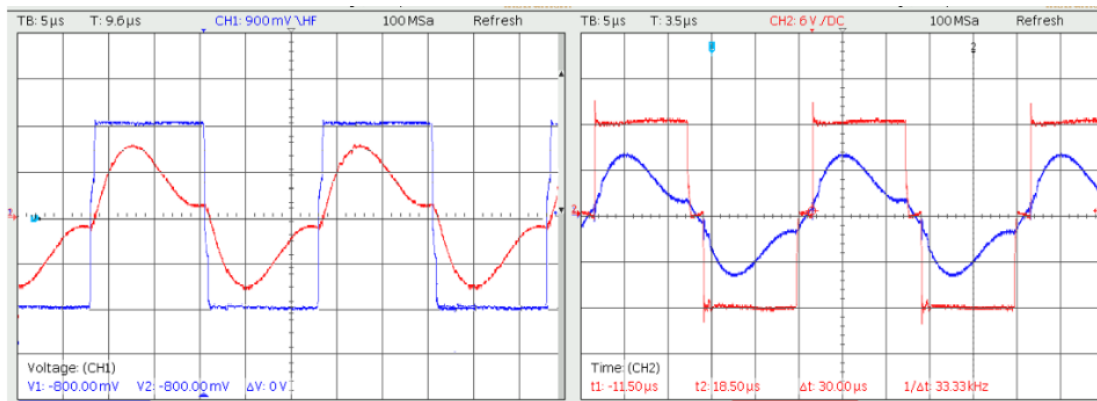


Figure 9. The voltage/current waveform of inverter in CC charging mode

## 4.2. Experiment results

A wireless charging system with a 2.5kW has built in the laboratory as in Figure 8. Polypropylene film capacitors are used in compensation circuits to reduce losses and increase high current tolerance in high-frequency systems. C3M0280090D SICs are used to improve inverter efficiency.

The experimental result waveforms of inverter output voltage/current in CC charging mode are shown in Figure 9. During the CC charging process, current charging is maintained by 8.5A, the ZVS is achieved perfectly, the ZCS condition is also almost achieved. The maximum efficiency reaches 92.1% at 2.5 kW in the CC charging mode when the receiver and transmitter are aligned.

## 5. CONCLUSION

The paper proposes to perform a wireless charging system for e-bike. The double-sided LCC compensation circuit is designed that the advantage of high efficiency and resonant frequency regardless of the coupling coefficient and load. The CC/CV charging control is performed only from the transmitter side. Also, the paper proposes a simple method to estimate both the load and the coupling coefficient based on measured parameters such as RMS of resonant current and input DC power of the inverter. The simulation and experimental results verify the feasibility of the proposed method. A 2.5 kW wireless charging system is built. The maximum charging efficiency reaches 92.1%.

## ACKNOWLEDGEMENTS

This research is funded by the Hanoi University of Science and Technology (HUST) under project number T2018-PC-054.

## REFERENCES

- [1] V. Kindl, R. Pechanek, M. Zavrel, and T. Kavalir, "Inductive coupling system for E-bike wireless charging," in *2018 ELEKTRO*, Mikulov, May 2018, pp. 1–4.

- [2] D. Iannuzzi, L. Rubino, L. P. Di Noia, G. Rubino, and P. Marino, "Resonant inductive power transfer for an E-bike charging station," *Electric Power Systems Research*, vol. 140, pp. 631–642, Nov. 2016.
- [3] F. Pellitteri, M. Caruso, V. Castiglia, R. Miceli, C. Spataro, and F. Viola, "Experimental Investigation on Magnetic Field Effects of IPT for Electric Bikes," *Electric Power Components and Systems*, vol. 46, no. 2, pp. 125–134, Jan. 2018.
- [4] Z. Bi, T. Kan, C. C. Mi, Y. Zhang, Z. Zhao, and G. A. Keoleian, "A review of wireless power transfer for electric vehicles: Prospects to enhance sustainable mobility," *Applied Energy*, vol. 179, pp. 413–425, Oct. 2016.
- [5] S. Li and C. C. Mi, "Wireless Power Transfer for Electric Vehicle Applications," *IEEE Journal of Emerging and Selected Topics in Power Electronics*, vol. 3, no. 1, pp. 4–17, Mar. 2015.
- [6] D. M. Vilathgamuwa and J. P. K. Sampath, "Wireless Power Transfer (WPT) for Electric Vehicles (EVs)—Present and Future Trends," in *Plug In Electric Vehicles in Smart Grids*, S. Rajakaruna, F. Shahnia, and A. Ghosh, Eds. Singapore: Springer Singapore, 2015, pp. 33–60.
- [7] C.-S. Wang, G. A. Covic, and O. H. Stielau, "Investigating an LCL Load Resonant Inverter for Inductive Power Transfer Applications," *IEEE Trans. Power Electron.*, vol. 19, no. 4, pp. 995–1002, Jul. 2004.
- [8] U. K. Madawala and D. J. Thrimawithana, "A Bidirectional Inductive Power Interface for Electric Vehicles in V2G Systems," *IEEE Transactions on Industrial Electronics*, vol. 58, no. 10, pp. 4789–4796, Oct. 2011.
- [9] Z. Pantic, S. Bai, and S. M. Lukic, "ZCS  $\$LCC\$$ -Compensated Resonant Inverter for Inductive-Power-Transfer Application," *IEEE Transactions on Industrial Electronics*, vol. 58, no. 8, pp. 3500–3510, Aug. 2011.
- [10] S. Li, W. Li, J. Deng, T. D. Nguyen, and C. C. Mi, "A Double-Sided LCC Compensation Network and Its Tuning Method for Wireless Power Transfer," *IEEE Transactions on Vehicular Technology*, vol. 64, no. 6, pp. 2261–2273, Jun. 2015.
- [11] T. Kan, T.-D. Nguyen, J. C. White, R. K. Malhan, and C. C. Mi, "A New Integration Method for an Electric Vehicle Wireless Charging System Using LCC Compensation Topology: Analysis and Design," *IEEE Trans. Power Electron.*, vol. 32, no. 2, pp. 1638–1650, Feb. 2017.
- [12] Sizhao Lu, Xiaoting Deng, Wenbin Shu, Xiaochao Wei, and Siqi Li, "A New ZVS Tuning Method for Double-Sided LCC Compensated Wireless Power Transfer System," *Energies*, vol. 11, no. 2, p. 307, Feb. 2018.
- [13] A. F. A. Aziz, M. F. Romlie, and T. Z. A. Zulkifli, "CLL/S Detuned compensation network for electric vehicles wireless charging application," *International Journal of Power Electronics and Drive Systems (IJPEDES)*, vol. 10, no. 4, pp. 2173–2181, Dec. 2019.
- [14] Weixiang Shen, Thanh Tu Vo, and A. Kapoor, "Charging algorithms of lithium-ion batteries: An overview," in *2012 7th IEEE Conference on Industrial Electronics and Applications (ICIEA)*, Jul. 2012, pp. 1567–1572.
- [15] K. Na, H. Ma, G. Namgoong, K. A. Kim, J.-H. Jung, and F. Bien, "Step-charging technique for CC/CV mode battery charging with low-cost control components in IPT systems," *IET Power Electronics*, vol. 11, no. 15, pp. 2523–2530, Dec. 2018.
- [16] J. M. Miller, O. C. Onar, and M. Chinthavali, "Primary-Side Power Flow Control of Wireless Power Transfer for Electric Vehicle Charging," *IEEE J. Emerg. Sel. Topics Power Electron.*, vol. 3, no. 1, pp. 147–162, Mar. 2015.
- [17] B. Pang, J. Deng, P. Liu, and Z. Wang, "Secondary-side power control method for double-side LCC compensation topology in wireless EV charger application," in *IECON 2017 - 43rd Annual Conference of the IEEE Industrial Electronics Society*, Beijing, Oct. 2017, pp. 7860–7865.
- [18] T. Diekhans and R. W. De Doncker, "A Dual-Side Controlled Inductive Power Transfer System Optimized for Large Coupling Factor Variations and Partial Load," *IEEE Trans. Power Electron.*, vol. 30, no. 11, pp. 6320–6328, Nov. 2015.
- [19] D. H. Tran, V. B. Vu, and W. Choi, "Design of a High-Efficiency Wireless Power Transfer System with Intermediate Coils for the On-Board Chargers of Electric Vehicles," *IEEE Trans. Power Electron.*, vol. 33, no. 1, pp. 175–187, Jan. 2018.
- [20] M. Kim, D. Joo, and B. K. Lee, "Design and Control of Inductive Power Transfer System for Electric Vehicles Considering Wide Variation of Output Voltage and Coupling Coefficient," *IEEE Transactions on Power Electronics*, vol. 34, no. 2, pp. 1197–1208, Feb. 2019.
- [21] S. Varikkottil and J. L. F. Daya, "Estimation of Optimal Operating Frequency for Wireless EV Charging System under Misalignment," *Electronics*, vol. 8, no. 3, p. 342, Mar. 2019.
- [22] R. Mai, Y. Chen, Y. Li, Y. Zhang, G. Cao, and Z. He, "Inductive Power Transfer for Massive Electric Bicycles Charging Based on Hybrid Topology Switching with a Single Inverter," *IEEE Transactions on Power Electronics*, vol. 32, no. 8, pp. 5897–5906, Aug. 2017.
- [23] Y. Chen, H. Zhang, S.-J. Park, and D.-H. Kim, "A Switching Hybrid LCC-S Compensation Topology for Constant Current/Voltage EV Wireless Charging," *IEEE Access*, vol. 7, pp. 133924–133935, 2019.
- [24] V.-B. Vu, D.-H. Tran, and W. Choi, "Implementation of the Constant Current and Constant Voltage Charge of Inductive Power Transfer Systems with the Double-Sided LCC Compensation Topology for Electric Vehicle Battery Charge Applications," *IEEE Trans. Power Electron.*, vol. 33, no. 9, pp. 7398–7410, Sep. 2018.
- [25] K. Song, Z. Li, J. Jiang, and C. Zhu, "Constant Current/Voltage Charging Operation for Series-Series and Series-Parallel Compensated Wireless Power Transfer Systems Employing Primary-Side Controller," *IEEE Trans. Power Electron.*, pp. 1–1, 2017.
- [26] Zhongming Ye, P. K. Jain, and P. C. Sen, "A Full-Bridge Resonant Inverter with Modified Phase-Shift Modulation for High-Frequency AC Power Distribution Systems," *IEEE Trans. Ind. Electron.*, vol. 54, no. 5, pp. 2831–2845, Oct. 2007.

**BIOGRAPHIES OF AUTHORS**

Nguyen Thi Diep received the B.E degree and M.S degree from the Hanoi University of Science and Technology, Hanoi, Vietnam, in 2004 and 2008. She is currently working toward the Ph.D. degree in the Hanoi University of Science and Technology, Hanoi, Vietnam. She works as a lecturer at Electric Power University.

Her research interests include wireless power transfer, wireless charging for EV, and power electronics.



Nguyen Kien Trung was born in Hanoi, Vietnam. He received the B.E. and M.Sc. degrees in control and automation from Hanoi University of Science and Technology, Vietnam in 2008 and 2011, respectively. In 2016, he received the Ph.D. degree in Functional control systems at Shibaura Institute of Technology, Japan, where he worked as a postdoctoral researcher in 2016-2017. From 2018, he works as a lecturer at Hanoi University of Science and Technology. Dr. Trung is a member of the IEEE and IEE of Japan.

His research interests include high-frequency converters and wireless power transfer systems.



Tran Trong Minh received the Ph.D. degree from Hanoi University of Science and Technology, Vietnam in 2008. Now, he works as a lecturer at Hanoi University of Science and Technology.

His research interests include power electronics, wireless power transfer systems.